Summer Student Report 2024

An analytical description of the saturation stage of the self-modulation instability in proton-driven plasma wakefield accelerators

González Manzano, Álvaro[1]

[1]Universidad de Sevilla

Friday 4th October, 2024

Supervisor: Moreira Mariana mariana.moreira@cern.ch

Keywords: plasma, wakefield, self-modulation instability, linear wakefield theory,

Abstract :

The goal of this work is to provide an analytical description of the saturation or nonlinear stage of the self-modulation instability (SMI), a critical phenomenon in oscillating unstable systems. In many such systems, the nonlinear stage is marked by a shift in the resonant frequency, which begins to depend on the amplitude of oscillation. This amplitude dependence fundamentally alters the system's behavior, leading to complex dynamics. To investigate this, we propose introducing a dependence of the resonant frequency, k_p, on the oscillation amplitude, specifically using the plasma density perturbation, δn as a key parameter. To approach this problem, we utilize the Green's function method in cases where the operator of the differential equation remains linear. With this we accomplish to model a realistic behaviour of the plasma density perturbation when the SMI goes through the saturation stage. The oscillations of the perturbation of the plasma density takes longer to disappear as the density spread of the bunch increases.

Contents

Introduction

Nowadays the pursuit of higher-energy accelerators is being impaired by the breakdown limit of the materials used for acceleration in conventional accelerators, among other technical hurdles. In order to achieve higher energy levels we need stronger magnetic and electric fields which require technologies that we do not have at the moment are simply expensive. This is why projects like AWAKE (Advanced WAKEfield Experiment) are so interesting for the future of high-energy physics. AWAKE aims to achieve acceleration gradients of approximately 300 MV/m by the end of its Run$\sim$ 2. In this experiment we use the wakefields generated in a plasma to accelerate an electron bunch. As a plasma is an ionized medium we do not have to worry about material breakdowns. Although a plasma carries other difficulties, such as instabilities and nonlinear effects, which can be challenging to describe analytically. The goal of this project is to describe one of those non-linear effects analytically. In particular, we seek the description of the self-modulation instability at its saturation stage, where a linear wakefield model is not valid anymore.

1 Plasma wakefield acceleration

Plasma-based acceleration is an advanced technique for accelerating charged particles using plasma waves and the high electric fields they generate. We can distinguish two types of technologies: plasma wakefield acceleration (PWFA) and laser wakefield acceleration (LWFA). PWFA is based on the use of a particle beam as a driver to generate a plasma wave, while LWFA uses a powerful laser pulse.

Plasma waves consist of a fluctuation of the plasma electron density and they provide the perfect structure to contain the particles we want to accelerate. Two common approximations are to consider that the heavier positive ions in the plasma are immobile, and that both species (ions and electrons) are cold (no thermal effects on particle motion). Under these conditions, disturbed plasma electrons oscillate at the plasma frequency, given by $\omega_p = \sqrt{e^2 n_0/\varepsilon_0 m_e}$ where n_0 is the plasma density, e is the elementary charge, ε_0 is the vacuum permittivity, and m_e is the electron mass, and thus form a plasma wave.

When a relativistic electron beam, for example, moves through plasma, it repels and disturbs the plasma electrons in its path. After the plasma electrons are repelled by the beam, they are pulled back by the positively charged ion column that remains, and they start to oscillate at ω_p. This collective oscillation forms a wave behind the electron bunch. The space charge separation of the oscillating plasma electrons and the static ion background translates into electric fields, with the plasma wake consisting of regions that can either accelerate or decelerate, and focus or defocus, particles.

Plasma-based acceleration is promising but faces significant challenges, especially in achieving high-quality particle bunches. These bunches need to have a high charge, maintain low emittance (which is a measure of the spread of particles in phase space), and exhibit minimal energy spread. Recent experimental results have shown progress in preserving these qualities, particularly in a specific regime called the blowout regime, where the plasma's focusing field depends linearly on the radius, which allows the emittance to be preserved.

However, controlling the energy spread of the accelerated particles remains difficult. In the linear regime, where the plasma density perturbation is smaller than the density of the driving bunch, the generated wakefields are sinusoidal and can introduce unwanted energy differences within the bunch. Techniques like beam loading, where the witness bunch has enough charge to drive its own wake and flatten the existing wakefields, especially if its profile is tailored specifically, can help reduce these issues.

In the blowout regime, the energy spread can be more predictable and might be corrected by further processing, potentially achieving very low energy spreads. Despite these ongoing challenges, significant progress was made in 2023 [1] when researchers demonstrated that plasma-accelerated electron bunches could be used in free-electron lasers, confirming the potential of plasma-based accelerators for advanced technological applications.

1.1 The self-modulation instability

In the linear regime, where the plasma density n_0 is much greater than the bunch density n_b, i.e., $n_0 \gg n_b$, the generated wakefields oscillate harmonically along the co-moving coordinate $\zeta = z - ct$ with a wavenumber $k_p = \omega_p/c$. For a long bunch, i.e., one that extends beyond one plasma wavelength $\lambda_p = 2\pi/k_p$, the action of the transverse component of the wakefields is felt by the bunch particles, thus periodically focusing and defocusing them. As the initial bunch profile is gradually shaped into a train of bunchlets with lengths and spacing of $\sim \lambda_p$, the plasma is disturbed at a frequency that is closer and closer to its natural resonant frequency ω_p. The wakefield amplitude therefore grows quasi-exponentially, and this feedback loop constitutes the self-modulation instability (SMI). Eventually, when all the bunch charge in defocusing regions has been lost, the instability enters a saturation stage.

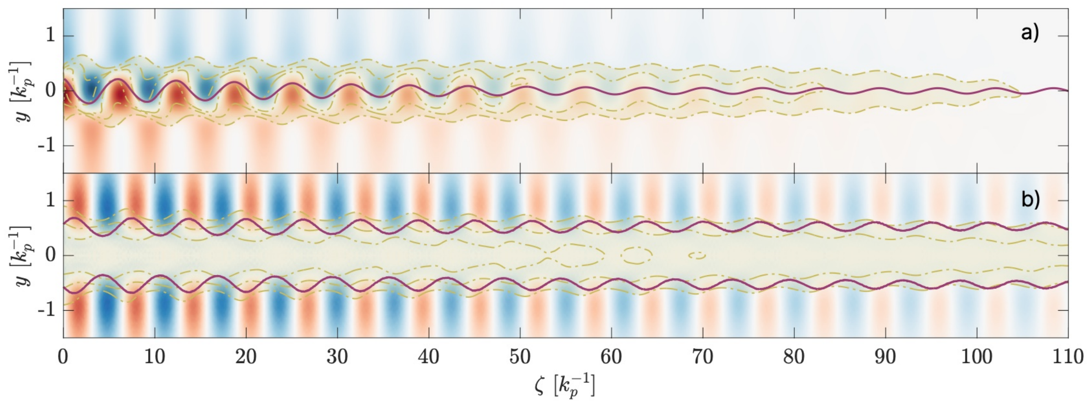

Figure 1: *Illustration of the so-called hosing instability (a) and the self-modulation instability (b). The blue-to-red color scale represents the transverse wakefield component, the yellow-shaded isosurfaces represent the bunch distribution, and the red solid lines represent the bunch centroid (a) and the RMS transverse bunch size (b).*[2]

Since the SMI is dictated by the transverse dynamics of the bunch particles, its evolution time scale is of the order of the betatron period $\omega_\beta^{-1} = \sqrt{2\gamma_b}/\omega_b$, with $\omega_b = \sqrt{n_{b0}q_b^2/(\varepsilon_0 M_b)}$ and where γ_b is the Lorentz factor of the bunch, n_{b0} is the peak bunch density, q_b is the bunch particle charge, and M_b is the bunch particle mass. The growth of the SMI has a spatiotemporal character, that is, the growth rate depends on both ζ and t (or z).

2 Theoretical Framework

In this section, our goal is to establish the mathematical tools and equations required to investigate the saturation stage of the self-modulation instability analytically.

2.1 A derivation of linear wakefield theory

Starting at the very beginning, we will use the Maxwell equations for electromagnetic fields and the cold fluid equations for both the plasma and the beam. The use of the cold fluid model is a good approximation when the thermal velocities of the plasma and beam particles are small compared to the plasma wake's phase velocity, which is approximately the speed of light. Moreover, we consider the plasma ions as stationary.

The Maxwell equations we are using are:

$$\nabla \cdot \vec{E} = 4\pi\rho \tag{1}$$

$$\nabla \cdot \vec{B} = 0 \tag{2}$$

$$\nabla \times \vec{E} = -\frac{1}{c}\frac{\partial \vec{B}}{\partial t} \tag{3}$$

$$\nabla \times \vec{B} = \frac{1}{c}\frac{\partial \vec{E}}{\partial t} + \frac{4\pi}{c}\vec{J} \tag{4}$$

where ρ and $\vec{J}$ are the charge and current density. As the plasma is composed of the sum of different species we can express them as:

$$\rho = \sum_{i=1}^{N} q_i n_i \tag{5}$$

$$\vec{J} = \sum_{i=1}^{N} q_i n_i \vec{v}_i \tag{6}$$

The relativistic cold fluid equation for each species are:

$$\frac{\partial n_i}{\partial t} + \nabla \cdot (n_i \vec{v}_i) = 0 \tag{7}$$

$$\left(\frac{\partial}{\partial t} + \vec{v}_i \cdot \nabla\right)\vec{p}_i = q_i\left(\vec{E} + \frac{\vec{v}_i}{c} \times \vec{B}\right) \tag{8}$$

$$\vec{p}_i = m_i \gamma_i \vec{v}_i \tag{9}$$

$$\gamma_i = \left(1 + \frac{p_i^2}{m_i^2 c^2}\right)^{\frac{1}{2}} \tag{10}$$

The Maxwell equations can be written in terms of the electric potential ϕ and the magnetic potential $\vec{A}$, using the following relations between the fields and the potentials:

$$\vec{B} = \nabla \times \vec{A} \tag{11}$$

$$\vec{E} = -\nabla\phi - \frac{1}{c}\frac{\partial \vec{A}}{\partial t} \tag{12}$$

It is also convenient to express these equations with normalized variables, in order to avoid carrying several constants. In our derivation we will use the following normalization:

$$
\begin{aligned}
\overline{r} &= k_p\vec{r} & \overline{t} &= \omega_p t \\
\bar{\vec{E}} &= e\vec{E}/m_e c\omega_p & \bar{\vec{B}} &= e\vec{B}/m_e c\omega_p \\
\bar{\vec{A}} &= e\vec{A}/m_e c^2 & \overline{\phi} &= e\phi/m_e c^2 \\
\overline{\rho} &= \rho/n_p e & \bar{\vec{J}} &= \vec{J}/n_p ec \\
\bar{\vec{v}}_i &= \vec{v}_i/c & \bar{\vec{p}}_i &= \vec{p}_i/m_e c \\
\overline{n}_i &= n_i/n_p & \overline{q}_i &= q_i/e \\
\overline{m}_i &= m_i/m_e & &
\end{aligned}
$$

With this we get:

$$\overline{\nabla} \cdot \bar{\vec{E}} = \overline{\rho} \tag{13}$$

$$\overline{\nabla} \cdot \bar{\vec{B}} = 0 \tag{14}$$

$$\overline{\nabla} \times \bar{\vec{E}} = -\frac{\partial\ \bar{\vec{B}}}{\partial \overline{t}} \tag{15}$$

$$\overline{\nabla} \times \bar{\vec{B}} = \frac{\partial\ \bar{\vec{E}}}{\partial \overline{t}} + \bar{\vec{J}} \tag{16}$$

$$\left(\frac{\partial^2}{\partial t^2} - \nabla^2\right) \bar{\vec{A}} = \bar{\vec{J}} \tag{17}$$

$$\left(\frac{\partial^2}{\partial t^2} - \nabla^2\right) \phi = \rho \tag{18}$$

$$\nabla \cdot \bar{\vec{A}} + \frac{\partial \phi}{\partial t} = 0 \tag{19}$$

$$\bar{\vec{B}} = \nabla \times \bar{\vec{A}} \tag{20}$$

$$\bar{\vec{E}} = -\nabla\phi - \frac{\partial \bar{\vec{A}}}{\partial t} \tag{21}$$

$$\rho = \sum_{i=1}^{N_i} q_i \bar{n}_i \tag{22}$$

$$\vec{J} = \sum_{i=1}^{N_i} q_i \bar{n}_i \vec{v}_i \tag{23}$$

$$\frac{\partial \bar{n}_i}{\partial t} + \nabla \cdot (\bar{n}_i \vec{v}_i) = 0 \tag{24}$$

$$\frac{\partial \vec{v}_i}{\partial t} + \vec{v}_i \cdot \nabla \vec{v}_i = \frac{q_i}{m_i}\left(\vec{E} + \vec{v}_i \times \vec{B}\right) \tag{25}$$

$$\left(\frac{\partial}{\partial t} + \vec{v}_i \cdot \nabla\right) \vec{p}_i = \frac{q_i}{m_i}\left(\vec{E} + \vec{v}_i \times \vec{B}\right) \tag{26}$$

$$\vec{p}_i = m_i \gamma_i \vec{v}_i \tag{27}$$

$$\gamma_i = \left(1 + \frac{p_i^2}{m_i^2 c^2}\right)^{\frac{1}{2}} \tag{28}$$

This set of equations is exceedingly cumbersome to solve. It is necessary to simplify the equations, firstly by changing the coordinates to a frame that moves along with the bunch as it propagates through the plasma, i.e., $(\overline{r}_\perp, \overline{z}, \overline{t}) \rightarrow (\overline{r}_\perp, s, \xi)$. This co-moving frame requires the following change of coordinates:

$$\xi = \overline{t} - \overline{z}$$
$$s = \overline{z}$$

The partial derivatives are transformed according to:

$$\frac{\partial}{\partial \overline{t}} = \frac{\partial}{\partial \xi} \qquad \frac{\partial}{\partial \overline{z}} = -\frac{\partial}{\partial \xi} + \frac{\partial}{\partial s}$$
$$\frac{\partial^2}{\partial \overline{t}^2} = \frac{\partial^2}{\partial \xi^2} \qquad \frac{\partial^2}{\partial \overline{z}^2} = \frac{\partial^2}{\partial \xi^2} - 2\frac{\partial}{\partial \xi}\frac{\partial}{\partial s} + \frac{\partial^2}{\partial s^2}$$

We decompose the vectors as follows:

$$\overline{S} = \overline{S}_\perp + \overline{S}_\parallel \hat{z}$$

where S represents a general vector quantity. After replacing all of these definitions, we obtain:

$$\nabla_\perp^2 \vec{A}_\perp = -\vec{J} \tag{29}$$
$$\nabla_\perp^2 \phi = -\rho \tag{30}$$
$$\nabla_\perp \cdot \vec{A}_\perp = -\frac{\partial}{\partial \xi}\left(\phi - A_\parallel\right) \tag{31}$$
$$\vec{E} = \vec{E}_\perp + E_\parallel \hat{z} \tag{32}$$
$$\vec{E}_\perp = -\nabla_\perp \phi - \frac{\partial \vec{A}_\perp}{\partial \xi} \tag{33}$$
$$E_\parallel = \frac{\partial}{\partial \xi}\left(\phi - A_\parallel\right) \tag{34}$$
$$\vec{B} = \vec{B}_\perp + B_\parallel \hat{z} \tag{35}$$
$$\vec{B}_\perp = \nabla_\perp \times \left(A_\parallel \hat{z}\right) + \nabla_\parallel \times \vec{A}_\perp \tag{36}$$
$$B_\parallel = \left(\nabla_\perp \times \vec{A}_\perp\right) \cdot \hat{z} \tag{37}$$
$$\frac{\partial}{\partial \xi}\left(\bar{n}_p - \bar{n}_p \vec{v}_{p\parallel}\right) + \nabla_\perp \cdot \left(\bar{n}_p \vec{v}_{p\perp}\right) = 0 \tag{38}$$
$$\left((1 - \vec{v}_{p\parallel})\frac{\partial}{\partial \xi} + \vec{v}_{p\perp} \cdot \nabla_\perp\right) \bar{p}_p = q_p \left(\vec{E} + \vec{v}_p \times \vec{B}\right) \tag{39}$$

Due to the very different time scales of the evolution of the beam and the plasma wake, we use the quasistatic approximation, where we essentially treat the beam as non-evolving during the time required for the plasma to respond to its presence, and then update the beam in s due to the plasma fields.

From the equations that link the potentials to the fields we can get the following set of equations:

$$\nabla_\perp^2 E_\perp = \nabla_\perp \rho + \frac{\partial J_\perp}{\partial \xi} \tag{40}$$
$$\nabla_\perp^2 E_\parallel = -\frac{\partial(\rho - J_\parallel)}{\partial \xi} \tag{41}$$
$$\nabla_\perp^2 B_\perp = -\nabla_\perp \times (J_\parallel \hat{z}) - \nabla_\parallel \times J_\perp \tag{42}$$
$$\nabla_\perp^2 B_\parallel = -(\nabla_\perp \times J_\perp) \cdot \hat{z} \tag{43}$$

These equations are the wave equations for the fields in the speed of light frame under the quasistatic approximation.

For the plasma electrons we have the following equations:

$$\frac{(n_e - n_e v_\parallel)}{\partial \xi} + \nabla_\perp \cdot n_e v_\perp = 0 \tag{44}$$

$$\left\{(1 - v_\parallel)\frac{\partial}{\partial \xi} + v_\perp \cdot \nabla_\perp\right\} p = -(E + v \times B) \tag{45}$$

where $p = \gamma v$ and $\gamma = (1 + p^2)^{1/2}$.

In order to make these equations tractable, we assume a small perturbation of the plasma density $n_e \to n + \delta n$, where n is a constant background plasma density and $\delta n \ll n$ is a small perturbation. This is valid when $n_b \ll n_e$. Then, omitting all the second or higher order terms in the equations presented above we get the following group of linearized equations:

$$\nabla_\perp^2 A_\perp = -J_\perp \tag{46}$$

$$\nabla_\perp^2 A_\parallel = -J_\parallel \tag{47}$$

$$\nabla_\perp^2 \phi = -\rho \tag{48}$$

$$\nabla_\perp \cdot A_\perp = -\frac{\partial}{\partial \xi}(\phi - A_\parallel) \tag{49}$$

$$J_\perp = -V_\perp \tag{50}$$

$$J_\parallel = -V_\parallel + q_b n_b \tag{51}$$

$$\rho = -n + q_b n_b \tag{52}$$

and the physical fields

$$E_\perp = -\nabla_\perp \phi - \frac{\partial A_\perp}{\partial \xi} \tag{53}$$

$$E_\parallel = \frac{\partial(\phi - A_\parallel)}{\partial \xi} \tag{54}$$

$$B_\perp = \nabla_\perp \times (A_\parallel \hat{z}) + \nabla_\parallel \times A_\perp \tag{55}$$

$$B_\parallel = (\nabla_\perp \times A_\perp) \cdot \hat{z} \tag{56}$$

After substituting the equations for ρ, $J_\perp$ and $J_\parallel$, the fields become:

$$\nabla_\perp^2 E_\perp = \nabla_\perp(-n + q_b n_b) - \frac{\partial V_\perp}{\partial \xi} \tag{57}$$

$$\nabla_\perp^2 E_\parallel = \frac{\partial(n - V_\parallel)}{\partial \xi} \tag{58}$$

$$\nabla_\perp^2 B_\perp = -\nabla_\perp \times (q_b n_b - V_\parallel)\hat{z} + \nabla_\parallel \times V_\perp \tag{59}$$

$$\nabla_\perp^2 B_\parallel = (\nabla_\perp \times V_\perp) \cdot \hat{z} \tag{60}$$

with the normalized plasma equations:

$$\frac{\partial}{\partial \xi}(n - V_{\parallel}) = -\nabla_{\perp} \cdot V_{\perp} \tag{61}$$

$$\frac{\partial V_{\perp}}{\partial \xi} = -E_{\perp} \tag{62}$$

$$\frac{\partial V_{\parallel}}{\partial \xi} = -E_{\parallel} \tag{63}$$

We can obtain two equations for the transverse and longitudinal electric fields, using equation (62) with (57) and (63) with (58):

$$\left(\nabla_{\perp}^2 - 1\right) E_{\perp} = \nabla_{\perp} \left(-\frac{\delta n}{n_0} + q_n n_b\right) \tag{64}$$

$$\left(\nabla_{\perp}^2 - 1\right) E_{\parallel} = \frac{\partial}{\partial \xi} \frac{\delta n}{n_0} \tag{65}$$

Note that the source term of the two equations are $\delta n / n_0$ and q_b / n_b, which means that we need a equation for $\delta n / n_0$. Taking the derivative of equation (61) and substituting it in equation (62) and (63), we get:

$$\frac{\partial^2}{\partial \xi^2} \frac{\delta n}{n_0} + \frac{\partial E_{\parallel}}{\partial \xi} = \nabla_{\perp} \cdot E_{\perp} \tag{66}$$

now substituting from (53) and (54), then using equations (30) and (31) we get:

$$\left(\frac{\partial^2}{\partial \xi^2} + 1\right) \frac{\delta n}{n_0} = q_b n_b \tag{67}$$

We now have the equations for δn, $E_{\perp}$ and $E_{\parallel}$. The procedure is as follows: first we solve the equation for δn, then we obtain $E_{\parallel}$, and eventually $E_{\perp}$.

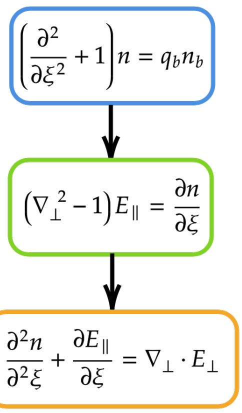

Figure 2: *Diagram of the procedure to obtain the transverse and longitudinal electric field and the plasma density perturbation.*

2.2 The Green's function method for solving linear differential equations

The Green's function method [3] allows us to solve differential equations of the kind

$$\mathcal{L}\phi(\mathbf{x}) = f(\mathbf{x}) \tag{68}$$

where $\mathcal{L}$ is a linear differential operator and the variable $\mathbf{x}$ is defined on the domain $\mathbf{x} \in \mathbf{D}$.

If we multiply this equation on both sides by $g(x, x')$, which will be our Green's function, and integrate them with respect to x from a to b:

$$\begin{gathered} g(x, x')\mathcal{L}\phi(\mathbf{x}) = g(x, x')f(\mathbf{x}) \rightarrow \\ \int_{\mathbf{D}} d\mathbf{x}\ g(\mathbf{x}, \mathbf{x}')\mathcal{L}\phi(\mathbf{x}) = \int_{\mathbf{D}} d\mathbf{x}\ g(\mathbf{x}, \mathbf{x}')f(\mathbf{x}) \end{gathered}$$

Using the Dirac notation for the inner product, we can write:

$$\langle g, \mathcal{L}\phi\rangle = \langle g, f\rangle \tag{69}$$

Now we take the adjoint, $\mathcal{L}^{adj}$, of the operator, $\mathcal{L}$:

$$\begin{gathered} \langle g, \mathcal{L}\phi\rangle = \langle \mathcal{L}^{adj} g, \phi\rangle + \text{boundary terms} \\ \langle \mathcal{L}^{adj} g, \phi\rangle = \langle g, f\rangle + \text{boundary terms} \end{gathered}$$

The boundary terms can be chosen such that they disappear and that the operator becomes self-adjoint, i.e., $\mathcal{L}^{adj}$. This choice in turn gives us some boundary conditions for the Green's function itself (which are required for its solution). By definition $g(\mathbf{x}, \mathbf{x}')$ satisfies:

$$\mathcal{L}^{adj} g(\mathbf{x}, \mathbf{x}') = \delta(\mathbf{x} - \mathbf{x}') \tag{70}$$

and therefore

$$\begin{gathered} \langle \mathcal{L}^{adj} g, \phi\rangle = \langle g, f\rangle \\ \langle \mathcal{L}^{adj} g, \phi\rangle = \langle \delta, \phi\rangle = \phi(\mathbf{x}') \end{gathered}$$

The solution to the differential equation (68) is therefore:

$$\phi(\mathbf{x}) = \int_{\mathbf{D}} d\xi\ g(\xi, \mathbf{x})f(\xi) \tag{71}$$

The solution requires that we first solve equation **(70)** and determine the Green's function $g(\mathbf{x}, \mathbf{x}')$.

In the last section we have obtained the equations for the plasma density and the longitudinal and transverse electric field, so our purpose now is to solve them using this method. In order to do so, we need to verify that the operator $\mathcal{L}$ is linear. This proof can be performed very easily with the homogeneity and additive properties:

- **Homogeneity:** $\mathcal{L}[\lambda f] = \lambda\mathcal{L}[f]$ where λ is a constant.

- **Additivity:** $\mathcal{L}[f + g] = \mathcal{L}[f] + \mathcal{L}[g]$

3 A theory for the saturation stage of the self-modulation instability

In the context of linear theory, it is typically assumed that both the plasma frequency and the plasma wavenumber, k_p, remain constant throughout the analysis. This simplification allows for more straightforward mathematical treatment of wave propagation in the plasma. However, this assumption does not fully capture the complexities of real plasma dynamics.

In reality, the plasma wavenumber k_p depends on the local plasma density. Since the plasma density is not uniform and can vary spatially and temporally, particularly as the SMI evolves, the assumption of a constant k_p becomes inadequate.

As the SMI progresses, local perturbations in the plasma density arise, which influence the plasma wavenumber. Therefore, to accurately model the system, it is necessary to account for the fact that k_p may change over time and space as a function of the evolving plasma density.

To incorporate this effect, we allow k_p to vary by explicitly linking it to the plasma density perturbation. This approach enables us to more realistically model the evolution of the system, capturing the dynamic interplay between the plasma wave and the evolving density structure as the SMI develops.

In a plasma the wavenumber of the wakefield oscillations of the electrons is related to the electron plasma frequency as follows:

$$k_p = \frac{\omega_p}{c} \tag{72}$$

where ω_p is the electron plasma frequency and c is the speed of light. We also know that ω_p is given by:

$$\omega_p = \sqrt{\frac{e^2 n_0}{\varepsilon_0 m_e}}$$

where e is the elementary charge; n_0 is the plasma density; ε_0 is the vacuum's permitivity; and m_e the electron's mass. Let us consider a small perturbation of the plasma, by writing the plasma density as $n_0 \to n_0 + \delta n$ and substituting it in the definition of the plasma wavenumber:

$$k_p = \frac{1}{c}\sqrt{\frac{e^2}{\varepsilon_0 m_e}(n_0+\delta n)} = \frac{1}{c}\sqrt{\frac{e^2 n_0}{\varepsilon_0 m_e}}\sqrt{\left(1+\frac{\delta n}{n_0}\right)} \simeq k_{p,0}\left(1+\frac{1}{2}\frac{\delta n}{n_0}\right)$$

We now have a linearized dependence of k_p on δn.

$$k_p \simeq k_{p,0}\left(1+\frac{1}{2}\frac{\delta n}{n_0}\right) \tag{73}$$

Then we insert this in the equation we obtained for the plasma density in section **1.1**, which is, before normalization:

$$\left(\frac{\partial^2}{\partial \xi^2}+k_p^2\right)\frac{\delta n}{n_0} = k_p^2 \frac{q_b n_b}{e n_0} \tag{74}$$

and we substitute the relation (73):

$$k_p^2 \simeq k_{p,0}^2\left(1+\cancelto{0}{\frac{1}{4}\frac{\delta n^2}{n_0^2}}+\frac{1}{2}\frac{\delta n}{n_0}\right) \to \frac{\partial^2}{\partial \xi^2}\frac{\delta n}{n_0}+k_{p,0}^2\left(1-\frac{q_b n_b}{e n_0}\right)\frac{\delta n}{n_0} = k_{p,0}^2\frac{q_b n_b}{e n_0}v$$

If we rearrange the equation and define $\delta\hat{n} := \delta n/n_0$ and the same for $n_b \to \hat{n}_b$ we get:

$$\frac{\partial^2}{\partial\xi^2}\delta\hat{n} + k_{p,0}^2\left(1+\hat{n}_b\right)\delta\hat{n} = -k_{p,0}^2\hat{n}_b \tag{75}$$

This is an inhomogeneous, linear, second-order differential equation with variable coefficients:

$$y''(x) + (1-f(x))y(x) + f(x) = 0 \tag{76}$$

Using the Green's function method explained in section 2.2 we can solve equation 76. First of all, we have to demonstrate the linearity of the operator $\mathcal{L}$, defined as:

$$\mathcal{L} = \frac{d^2}{dx^2} + (1-f(x)) \tag{77}$$

If $\mathcal{L}$ is linear, it must satisfy:

- **Homogeneity:**

$$\begin{aligned}\mathcal{L}\left[\lambda g\right] &= \frac{d^2(\lambda g)}{dx^2} + (1-f(x))\left(\lambda g\right) = \\ &= \lambda\left[\frac{d^2 g}{dx^2} + (1-f(x))\,g\right] = \\ &= \lambda\mathcal{L}\left[g\right]\end{aligned}$$

- **Additivity:**

$$\begin{aligned}\mathcal{L}\left[g+h\right] &= \frac{d^2}{dx^2}(g+h) + (1-f(x))\left(g+h\right) = \\ &= \frac{d^2 g}{dx^2} + (1-f(x))\,g + \frac{d^2 h}{dx^2} + (1-f(x))\,h = \\ &= \mathcal{L}\left[g\right] + \mathcal{L}\left[h\right]\end{aligned}$$

As we can see, $\mathcal{L}$ is linear, so we can apply the Green's function method to solve the equation

$$\mathcal{L}y(x) = f(x) \tag{78}$$

In order to do so, we present two strategies. First we consider the simplest scenario, in which $f(x) = \text{const}$. This assumption may be valid when we consider the center of a long bunch profile ($\sigma_z \gg \lambda_p$), where the longitudinal profile can be approximated as $\approx n_{b0}$. Then we solve the general problem, where $f(x)$ is a function.

3.1 Case 1: $f(x) = -C$

In this case our differential operator is:

$$\mathcal{L} := \frac{d^2}{dx^2} + (1+C)$$

and the differential equation we must resolve is:

$$\mathcal{L}y(x) = -C$$

We proceed with the Green's Function method, then the solution of this problem is:

$$y(x') = -C \int_{x'}^{\infty} dx g(x, x')$$

And for the green's function we have the equation:

$$\mathcal{L}g(x, x') = \delta(x - x')$$

It is easy to find that in this case $\mathcal{L} = \mathcal{L}^{\text{adj}}$.

In order to solve this we divide it in two reegions:

$$\mathcal{L}g(x, x') = \delta(x - x') \Rightarrow \begin{cases} \frac{\partial^2 g(x,x')}{\partial^2 x} + (1 + C)g(x, x') = 0 & x < x' \\ \frac{\partial^2 g(x,x')}{\partial^2 x} + (1 + C)g(x, x') = 0 & x > x' \end{cases}$$

The general solution for a differential equation of the form:

$$g''(x, x') + (1 + C)g(x, x') = 0$$

is

$$g(x, x') = A \sin\left(\sqrt{1 + C}\ x\right) + B \cos\left(\sqrt{1 + C}\ x\right)$$

Now if we impose the boundary conditions and the continuity consitions for the green's function:

$$g(x, x') = \begin{cases} 0 & x < x' \\ \frac{1}{\sqrt{1+C}} \sin\left(\sqrt{1 + C}\ (x - x')\right) & x > x' \end{cases}$$

Then our solution will be

$$y(x) = \frac{C}{\sqrt{1 + C}} \int_{x}^{\infty} dx'\ \sin\left(\sqrt{1 + C}\ (x' - x)\right)$$

This solution shows a sinusoidal behaviour and tells us that the density perturbation of the plasma density oscillates as a sinusoid once the constant density charged bunch interrupts in the plasma.

3.2 Case 2: $f(x) \neq C$

Now $f(x) \neq C$ and the operator is:

$$\mathcal{L} = \frac{d^2}{dx^2} + (1 - f(x))$$

But as we demonstrated this is still linear and we can apply the green's method. So by redoing all the steps did before we reach to a similar equation:

$$y(x') = \int_{x'}^{\infty} dx\ g(x, x')f(x)$$

As before, in order to solve this we must solve first

$$\mathcal{L}g(x, x') = \delta(x - x')$$

In this case the problem splits as follows

$$g(x,x') = \begin{cases} \frac{d^2g}{dx} + (1-f(x))g(x,x') = 0 & x < x' \\ \frac{d^2g}{dx} + (1-f(x))g(x,x') = 0 & x > x' \end{cases}$$

Just to simplify the calculations we define $h(x) := 1 - f(x)$ and the differential equation we must to resolve is:

$$g''(x,x') + h(x)g(x,x') = 0$$

3.2.1 Particular Case:

We could think analytically using a gaussian function is better than others, but for our purpose it seems a better option to use a cosine function with a RMS equivalent to the gaussian, but with the advantage of being exactly zero for any other range. Also this is more realistic as the density of the bunch of particles does not decrease to infinity:

$$f(x) = \begin{cases} \frac{1}{2}\left[1 - \cos\left(\sqrt{\frac{\pi}{2}}\frac{x}{\sigma}\right)\right] & 0 < x < 2\sqrt{2\pi}\sigma \\ 0 & x > 2\sqrt{2\pi}\sigma \end{cases} \tag{79}$$

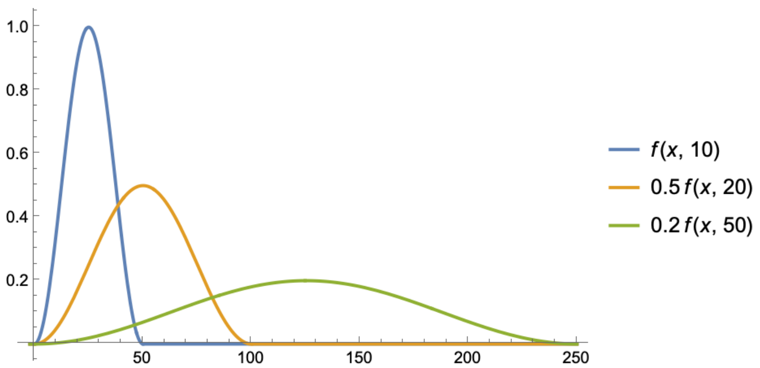

Figure 3: $f(x)$ representation for different values of σ keeping constant the bunch's charge.

Changing this particular case in our differential equation for the green's function we get:

$$g(x,x') = \begin{cases} \frac{d^2g}{dx} + \left[\frac{1}{2} - \frac{1}{2}\cos\left(\sqrt{\frac{\pi}{2}}\frac{x}{\sigma}\right)\right] g(x,x') = 0 & 0 < x < x' \\ \frac{d^2g}{dx} + \left[\frac{1}{2} - \frac{1}{2}\cos\left(\sqrt{\frac{\pi}{2}}\frac{x}{\sigma}\right)\right] g(x,x') = 0 & x' < x < 2\sqrt{2\pi}\sigma \\ \frac{d^2g}{dx} + g(x,x') = 0 & 2\sqrt{2\pi}\sigma < x < x' \\ \frac{d^2g}{dx} + g(x,x') = 0 & x' < x \end{cases}$$

With the boundary conditions:

$$\textbf{BCs: } y(x \to \infty) = 0 \qquad \left.\frac{\partial y}{\partial x}\right|_{x\to\infty} = 0$$

$$\textbf{GBCs: } g(0,x') = 0 \qquad \left.\frac{\partial g(x,x')}{\partial x}\right|_{x=0} = 0$$

$$\textbf{GCCs: } \lim_{\varepsilon\to 0} g(x'+\varepsilon,x') = \lim_{\varepsilon\to 0} g(x'-\varepsilon,x') \qquad \partial_x g(x,x')\big|_{x=x'+\varepsilon} - \partial_x g(x,x')\big|_{x=x'-\varepsilon} = 1$$

First we will rewrite the equation for the interval from 0 to $2\sqrt{2\pi}\sigma$. The equation is:

$$\frac{d^2g}{dx} + \left[\frac{1}{2} - \frac{1}{2}\cos\left(\sqrt{\frac{\pi}{2}}\frac{x}{\sigma}\right)\right] g(x,x') = 0$$

we will introduce the change of coordinates:

$$2\eta = \frac{x}{\sigma}\sqrt{\frac{\pi}{2}} \rightarrow x = 2\sigma\sqrt{\frac{2}{\pi}}\eta \qquad\qquad \frac{\partial}{\partial x} = \frac{1}{2\sigma}\sqrt{\frac{\pi}{2}}\frac{\partial}{\partial \eta}$$

then the differential equation turns into:

$$\frac{1}{4\sigma^2}\frac{\pi}{2}\frac{\partial^2 g}{\partial \eta^2} + \frac{1}{2}\left[1 - cos(2\eta)\right] g = 0 \Rightarrow \frac{\partial^2 g(\eta,\eta')}{\partial \eta^2} + \left[a - 2q\cos\left(2\eta\right)\right] g(\eta,\eta') = 0$$

which is the **Mathieu's differential equation**[4] for:

$$\alpha = \frac{1}{2\sigma}\sqrt{\frac{\pi}{2}} \qquad\qquad a = (1 - \hat{n}_{b0})\frac{1}{\alpha^2} \qquad\qquad q = -\frac{\hat{n}_{b_0}}{4\alpha^2}$$

The solution for this equation are the **Mathieu's functions**, for each interval will be:

$$\begin{aligned} g(\eta,\eta') &= c_1\mathbf{C}(a,q,\eta) + c_2\mathbf{S}(a,q,\eta) && 0 < \eta < \eta' \\ g(\eta,\eta') &= c_3\mathbf{C}(a,q,\eta) + c_4\mathbf{S}(a,q,\eta) && \eta' < \eta < \pi \end{aligned}$$

The equivalence between coordinates can be more clearly seen in this picture:

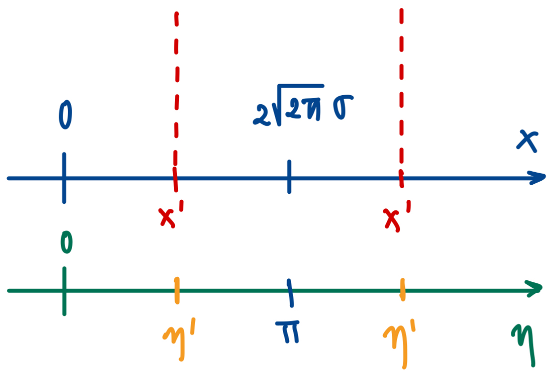

Figure 4: Interval for the green's function for x coordinate (up) and η coordinate (down)

At this point we use the boundary conditions:

$$\begin{aligned} &\mathbf{GBCs} \rightarrow g(\eta,\eta') = c_1\mathbf{C}(a,q,\eta) + c_2\mathbf{S}(a,q,\eta) \Rightarrow c_1 = c_2 = 0 && 0 < \eta < \eta' \\ &\mathbf{GCCs} \rightarrow g(\eta,\eta') = c_3\mathbf{C}(a,q,\eta) + c_4\mathbf{S}(a,q,\eta) \Rightarrow c_3, c_4 && \eta' < \eta < \pi \end{aligned}$$

It can be shown that the coefficients c_3 and c_4 are then:

$$c_3(a,q,\eta') = \frac{2\sigma\sqrt{2/\pi}}{\mathbf{S}'(a,q,\eta') - \frac{\mathbf{S}(a,q,\eta')}{\mathbf{C}(a,q,\eta')}\mathbf{C}'(a,q,\eta')} \qquad c_4(a,q,\eta') = \frac{2\sigma\sqrt{2/\pi}}{\mathbf{C}'(a,q,\eta') - \frac{\mathbf{C}(a,q,\eta')}{\mathbf{S}(a,q,\eta')}\mathbf{S}'(a,q,\eta')}$$

For the cases $\pi < \eta < \eta'$ and $\eta' < \eta$, we have:

$$\begin{aligned} g(\eta,\eta') &= c_5\sin 2\sigma\sqrt{\frac{2}{\pi}}\eta + c_6\cos 2\sigma\sqrt{\frac{2}{\pi}}\eta && \pi < \eta < \eta' \\ g(x,x') &= c_7\sin 2\sigma\sqrt{\frac{2}{\pi}}\eta + c_8\cos 2\sigma\sqrt{\frac{2}{\pi}}\eta && \eta' < \eta \end{aligned}$$

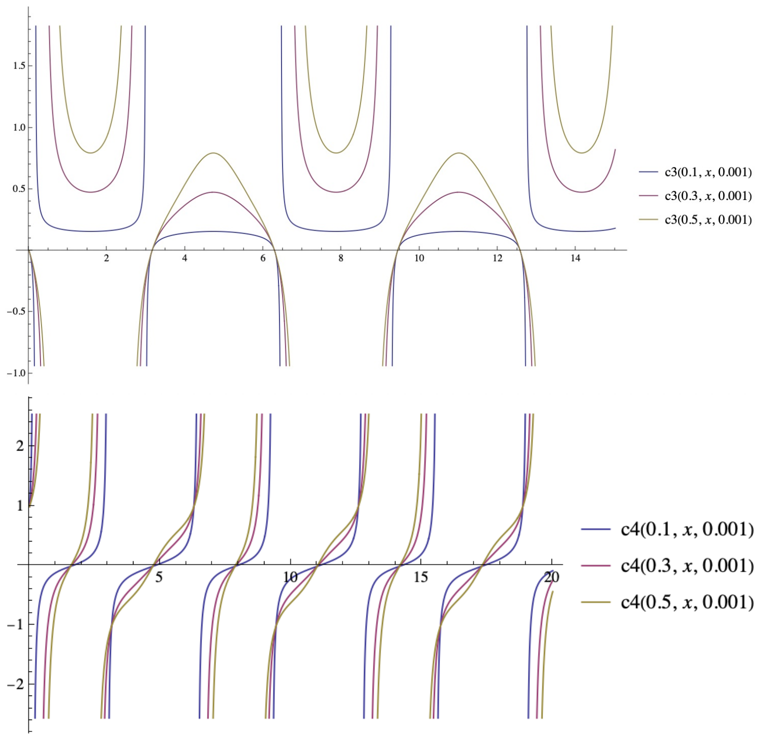

Figure 5: In this picture we plotted the coefficients c_3 and c_4 for different values of σ.

and if we use the boundary conditions:

$$g(\pi,\eta')^+ = g(\pi,\eta')^- \qquad \partial_x g(\pi,\eta')^+ - \partial_x g(\pi,\eta')^- = 2\sigma\sqrt{\frac{2}{\pi}}$$

$$g(\eta',\eta')^+ = g(\eta',\eta')^- \qquad \partial_x g(\pi,\eta')^+ - \partial_x g(\pi,\eta')^- = 2\sigma\sqrt{\frac{2}{\pi}}$$

Then the coefficients c_5, c_6, c_7, c_8:

$$c_5 = \sin(2\sigma\sqrt{2\pi})\,[c_3\mathbf{C}(a,q,\pi) + c_4\mathbf{S}(a,q,\pi)] + \frac{\cos(2\sigma\sqrt{2\pi})}{2\sigma}\sqrt{\frac{\pi}{2}}\left[2\sigma\frac{2}{\pi} + c_3\mathbf{C'}(a,q,\pi) + c_4\mathbf{S'}(a,q,\pi)\right]$$

$$c_6 = \cos(2\sigma\sqrt{2\pi})\,[c_3\mathbf{C}(a,q,\pi) + c_4\mathbf{S}(a,q,\pi)] + \frac{\sin(2\sigma\sqrt{2\pi})}{2\sigma}\sqrt{\frac{\pi}{2}}\left[2\sigma\frac{2}{\pi} + c_3\mathbf{C'}(a,q,\pi) + c_4\mathbf{S'}(a,q,\pi)\right]$$

$$c_7 = c_5 + \cos\left(2\sigma\sqrt{\frac{2}{\pi}}\right)$$

$$c_8 = c_6 - \sin\left(2\sigma\sqrt{\frac{2}{\pi}}\right)$$

with this the green's function is:

$$g(\eta,\eta') = \begin{cases} 0 & 0<\eta<\eta' \\ c_3\mathbf{C}(a,q,\eta) + c_4\mathbf{S}(a,q,\eta) & \eta'<\eta<\pi \\ c_5\sin\left(2\sigma\sqrt{\frac{2}{\pi}}\eta\right) + c_6\cos\left(2\sigma\sqrt{\frac{2}{\pi}}\eta\right) & \pi<\eta<\eta' \\ c_7\sin\left(2\sigma\sqrt{\frac{2}{\pi}}\eta\right) + c_8\cos\left(2\sigma\sqrt{\frac{2}{\pi}}\eta\right) & \eta'<\eta \end{cases} \tag{80}$$

Finally the solution we are looking for is:

$$y(\eta) = \int_{\eta}^{\pi} d\eta' \left[c_3(a,q,\eta)\mathbf{C}(a,q,\eta') + c_4(a,q,\eta)\mathbf{S}(a,q,\eta')\right] \frac{1}{2}\left[1 - \cos 2\eta'\right]$$

Seems pretty clear that this integral can not be solve by hand, so we solved it using *Wolfram Mathematica*. The full expression is:

$$y(\eta) = \frac{\sigma\sqrt{2/\pi}}{\mathbf{S}'(a,q,\eta) - \frac{\mathbf{S}(a,q,\eta)}{\mathbf{C}(a,q,\eta)}\mathbf{C}'(a,q,\eta)} \int_{\eta}^{\pi} d\eta' \mathbf{C}(a,q,\eta)\left[1 - \cos 2\eta'\right] +$$
$$+ \frac{\sigma\sqrt{2/\pi}}{\mathbf{C}'(a,q,\eta) - \frac{\mathbf{C}(a,q,\eta)}{\mathbf{S}(a,q,\eta)}\mathbf{S}'(a,q,\eta)} \int_{\eta}^{\infty} d\eta' \mathbf{S}(a,q,\eta)\left[1 - \cos 2\eta'\right]$$

The plot obtained is:

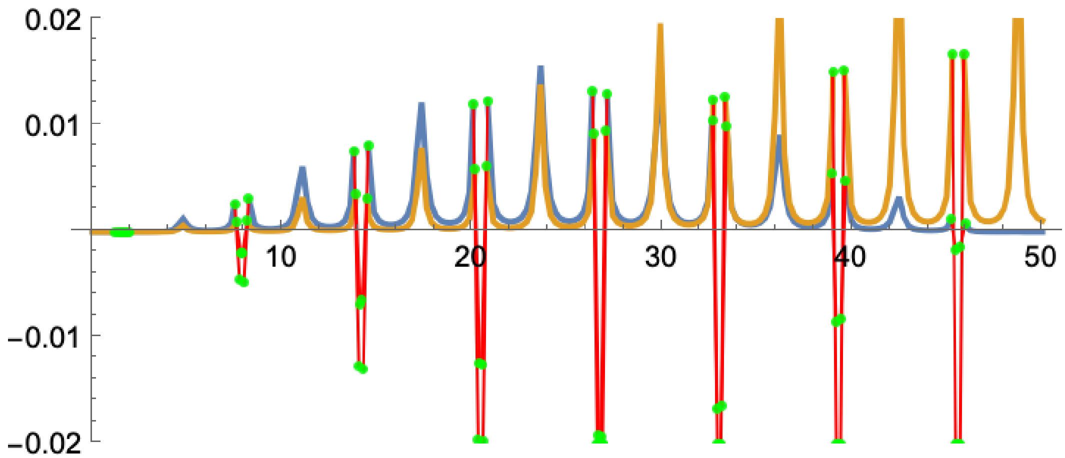

Figure 6: *Full solution for different values of* σ *and for* $n_b = 0.001$ *fixed. The horizontal axix represents the spatial coordinate along the bunch's path. And the vertical axis, the variation of the plasma density.*

As we can see in the plot. The smaller the bunch spread the faster the instability develops. The blue line correspond to the smaller value of $\sigma = 10$, we can see the instability grows quicker than the higher values. For example, for a $\sigma = 20$, the instability takes longer to disappear. The red and green lines are divergences caused by the numerical method that *Wolfram Mathematica* use to represent the **Mathieu's Functions**.

If we expand the domain of the plot we can see, as it was expected, that the orange solution for the higher value of σ follows the explained behavior.

The next plot shows the linear model. The main difference we can see is that the linear theory shows a non-decreasing behaviour of the oscillations of the plasma density variation, meanwhile our model establish a more realistic view as the variation of the plasma density starts and ends the oscillations. The blue line corresponds to a lower value of the argument of the sinusoids functions. This arguments relates to the charge density of the bunch which perturbs the plasma, it must be recalled that this solution started from assuming the bunch charge density is constant.

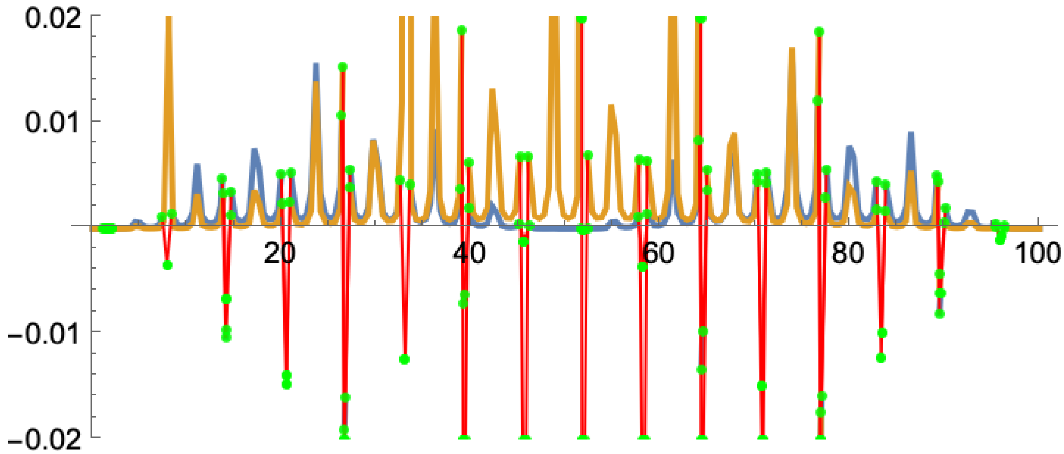

Figure 7: *Expanded domain for the solution in Figure* **(7)**.

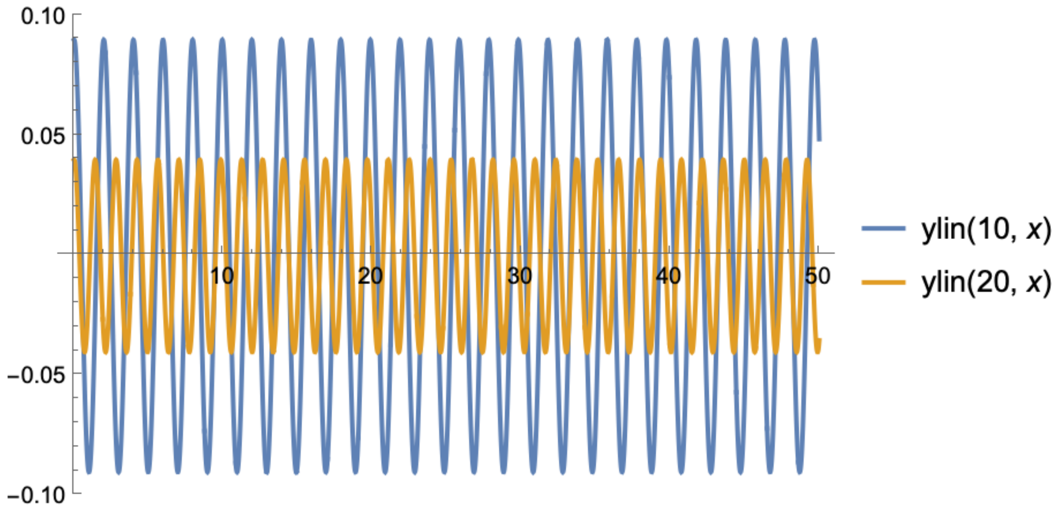

Figure 8: *Plot of the linear solution.*

3.2.2 General Case:

In this section we try to solve the differential equations for the Green's function for any $f(x)$ by doing a series expansion. The solution comes from assuming a function of the form of:

$$g(x, x') = \sum_{n=0}^{\infty} c_n (x - x')^n$$

and the same for the function $h(x)$, and then we get:

$$\sum_{n=0}^{\infty} c_{n+2}(n+2)(n+1)(x-x')^n + \sum_{n=0}^{\infty}\sum_{k=0}^{\infty} h_k c_n (x-x')^{n+k} = 0$$

Here we apply a little trick to have it in a more convenient form, and that is the following. If we have to functions $\alpha(x)$ and $\beta(x)$ that can be written as a series:

$$\alpha(x) = \sum_{n=0}^{\infty} a_n (x - x_0)^n \qquad \beta(x) = \sum_{n=0}^{\infty} b_n (x - x_0)^n$$

and we multiply them

$$\alpha(x)\cdot\beta(x) = \left(\sum_{n=0}^{\infty} a_n (x-x_0)^n\right)\left(\sum_{n=0}^{\infty} b_n (x-x_0)^n\right)$$

if we are inside the convergence radius we can use the distributive and commutative relations

$$\begin{aligned}\alpha(x)\cdot\beta(x) &= \sum_{n=0}^{\infty}\sum_{k=0}^{\infty} a_n b_k (x-x_0)^{n+k} = \\ &= \sum_{m=0}^{\infty} (x-x_0)^n \sum_{n=0}^{m} a_n b_{m-n} \\ &= \sum_{n=0}^{\infty} c_n (x-x_0)^n\end{aligned}$$

where we have defined

$$c_n := \sum_{k=0}^{n} a_k b_{n-k}$$

Then coming back to our equation, we get:

$$\sum_{n=0}^{\infty}\left[c_{n+2}(n+2)(n+1) + \sum_{k=0}^{n} c_k h_{n-k}\right](x-x')^n = 0$$

$$\sum_{n=0}^{\infty}\left[c_{n+2}(n+2)(n+1) + d_n\right](x-x')^n = 0$$

The coefficients keep to:

$$c_{n+2} = -\frac{d_n}{(n+2)(n+1)} = -\frac{\sum_{k=0}^{n} c_k h_{n-k}}{(n+2)(n+1)}$$

This recurrence relation is valid for all values of n, but we must give in advance a value for c_1 and c_0, which in order to do things easier we can take $c_1 = 0$, for c_0 we can give any number but zero, otherwise we end up with the trivial solution $g(x,x') = 0$, then:

$$c_2 = -\frac{c_0 h_0}{2} \qquad c_3 = -\frac{-c_0 a_1}{6} \qquad c_4 = -\frac{c_0 h_4}{12} + \frac{c_0 h_0 h_2}{24} \qquad \ldots$$

About the coefficients of $h(x)$ it wouldn't be a problem as we can usually expand the functions we commonly use as series with defined coefficients.

The final form of the solution will be:

$$y(x) = g(0,x)y'(0) - g'(0,x)y(0) + \int_0^{\infty} dx' \sum_{n=0}^{\infty} c_n (x'-x_0)^n f(x')$$

the coefficients c_n are obtained by using the recurrence relation previously deducted.

For a simple case in which $f(x) = e^{-x^2}$ and $x_0 = 0$ the solution can be calculated as it is shown[1]:

$$y(x) = \sum_{n=0}^{\infty} c_n \int_0^{\infty} dx' \ (x')^n e^{-(x')^2} =$$
$$= \sum_{n=0}^{\infty} \frac{1}{2} c_n \Gamma\left(\frac{n+1}{2}\right)$$

It can be shown that this solution is not divergent, as $n \to \infty$, $\Gamma((n+1)/2) \to \infty$, but $c_{n\to\infty} \to 0$, so

$$\left| \sum_{n=0}^{\infty} \frac{c_n}{2} \Gamma\left(\frac{n+1}{2}\right) \right| < \infty$$

3.3 Case 3: A daring attempt

First we define: $\mathcal{L} := d^2/dx^2 + A$ where A is a constant, and $U(x) = -(1+y(x))f(x)$, hence the so called equation turns to:

$$\mathcal{L}f(x) = U(x) \tag{81}$$

The next step is multiply equation (81) by $g(x,x')$ and integrate it from 0 to ∞:

$$\int_0^{\infty} dx \ g(x,x')\mathcal{L}y(x) = \int_0^{\infty} dx \ g(x,x')U(x)$$

now we expand the left-hand side of the equation, integrating by parts:

$$\int_0^{\infty} dx \ g(x,x')\mathcal{L}y(x) = \left[g(x,x')y'(x)\right]_0^{\infty} - \left[g'(x,x')y(x)\right]_0^{\infty} + \int_0^{\infty} dx \ \mathcal{L}g(x,x')y(x)$$

about the boundary conditions, we suppose that $y(x=0) = a_1$ as well as $y'(x=0) = a_2$, and later we will impose $g(\infty, x') = g'(\infty, x') = 0$. With this all, equation (81) can be rewritten as:

$$\int_0^{\infty} dx \ \mathcal{L}g(x,x')y(x) = \int_0^{\infty} dx \ g(x,x')U(x) - \left[g(x,x')y'(x)\right]_0^{\infty} + \left[g'(x,x')y(x)\right]$$

At this point we make our supposition of what does the green function must abide by. In our case we impose:

$$\mathcal{L}g(x,x') = \delta(x-x') \tag{82}$$

so we get:

$$\int_0^{\infty} dx \ \mathcal{L}g(x,x')y(x) = y(x') = \int_0^{\infty} dx \ g(x,x')U(x)$$

But we need to solve the equation we imposed for the green's function:

- for $x < x'$:
$$\frac{d^2 g(x,x')}{dx^2} + Ag(x,x') = 0$$
- and for $x > x'$:
$$\frac{d^2 g(x,x')}{dx^2} + Ag(x,x') = 0$$

[1]The integrals can be found in [5]

the general solutions for this differential equations is well known:

$$g(x,x') = \begin{cases} c_1 \sin\sqrt{A}x + c_2\cos\sqrt{A}x & x < x' \\ c_3 \sin\sqrt{A}x + c_4\cos\sqrt{A}x & x > x' \end{cases} \tag{83}$$

If we substitute the boundary conditions we get: $c_3 = c_4 = 0$. And for the solution when $x < x'$, we integrate the equation (82) from $x' - \varepsilon$ to $x' + \varepsilon$ and impose the continuity of $g(x, x')$:

$$\frac{d}{dx}g(x'+\varepsilon, x') - \frac{d}{dx}g(x'-\varepsilon, x') = 1 \tag{84}$$

$$g(x'+\varepsilon, x') - g(x'-\varepsilon, x') = 0 \tag{85}$$

this provides us two equation for finding the coefficients c_1 and c_2:

$$c_1 = \frac{\cos\sqrt{A}x'}{\sqrt{A}} \qquad\qquad c_2 = -\frac{\sin\sqrt{A}x'}{\sqrt{A}}$$

so our green function is:

$$g(x,x') = \begin{cases} \frac{\cos\sqrt{A}x'}{\sqrt{A}}\sin\sqrt{A}x - \frac{\sin\sqrt{A}x'}{\sqrt{A}}\cos\sqrt{A}x & x < x' \\ 0 & x > x' \end{cases} \tag{86}$$

Now we go back to our solution of the equation (81):

$$y(x) = a_2\frac{\sin\sqrt{A}x}{\sqrt{A}} + a_1\cos\sqrt{A}x + \int_0^x d\xi \left[\frac{\cos\sqrt{A}x'}{\sqrt{A}}\sin\sqrt{A}x - \frac{\sin\sqrt{A}x'}{\sqrt{A}}\cos\sqrt{A}x\right]U(\xi) \tag{87}$$

where we changed $x' \to x$ and $x \to \xi$ and $U(\xi) = -(1 - y(\xi))f(\xi)$.

The final solution of our problem depends on the solution to the integral at the right side of the equation (87). But as we can see the solution of the problem $y(x)$ is also inside the integral. If we consider that the effect of this term is small enough, we can find $y(x)$, assuming $y_0(x) = a_2\frac{\sin\sqrt{A}x}{\sqrt{A}} + a_1\cos\sqrt{A}x$ and putting this inside the integral:

$$I = -\int_0^x d\xi \left(\frac{\cos\sqrt{A}x'}{\sqrt{A}}\sin\sqrt{A}\xi - \frac{\sin\sqrt{A}x'}{\sqrt{A}}\cos\sqrt{A}\xi\right)\left(1 - a_2\frac{\sin\sqrt{A}\xi}{\sqrt{A}} - a_1\cos\sqrt{A}\xi\right)f(\xi)$$

We can define:

$$I_1 = \int_0^x d\xi\, \frac{\cos\sqrt{A}x'}{\sqrt{A}} f(\xi)\sin\sqrt{A}\xi \qquad I_2 = -\int_0^x d\xi\, \frac{\sin\sqrt{A}x'}{\sqrt{A}} f(\xi)\cos\sqrt{A}\xi$$

$$I_3 = -a_2\int_0^x d\xi\, \frac{\cos\sqrt{A}x'}{A} f(\xi)\sin^2(\sqrt{A}\xi) \qquad I_4 = -a_1\int_0^x d\xi\, \frac{\sin\sqrt{A}x'}{A} f(\xi)\cos^2(\sqrt{A}\xi)$$

$$I_5 = -a_1\int_0^x d\xi\, \frac{\cos\sqrt{A}x'}{\sqrt{A}} f(\xi)\sin\sqrt{A}\xi\cos\sqrt{A}\xi \qquad I_6 = -a_2\int_0^x d\xi\, \frac{\sin\sqrt{A}x'}{A} f(\xi)\sin\sqrt{A}\xi\cos\sqrt{A}\xi$$

hence $I = \sum_{n=1}^{6} I_n$.

For example, if we take a bunch with a gaussian density profile, i.e., $f(\xi) \sim e^{-\xi^2}$, and take all the constants $a_1 = a_2 = 1$ then[2]:

$$
\begin{aligned}
I_1 &= \frac{1}{4} e^{-\frac{\pi^2}{4}} \sqrt{\pi} \left(2\,\mathrm{Erfi}\left[\frac{\pi}{2}\right] - \mathrm{Erfi}\left[\frac{\pi}{2} + \mathrm{i}x\right] - \mathrm{Erfi}\left[\frac{1}{2}(\pi - 2\,\mathrm{i}x)\right]\right) \\
I_2 &= \frac{1}{4} \mathrm{i} e^{-\frac{A^2}{4}} \sqrt{\pi} \left(\mathrm{Erfi}\left[\frac{A}{2} - \mathrm{i}x\right] - \mathrm{Erfi}\left[\frac{A}{2} + \mathrm{i}x\right]\right) \\
I_3 &= \frac{1}{8} e^{-\pi^2} \sqrt{\pi} \left[2e^{\pi^2}\,\mathrm{Erf}(x) - \mathrm{i}\left(\mathrm{Erfi}(\pi - \mathrm{i}x) - \mathrm{Erfi}(\pi + \mathrm{i}x)\right)\right] \\
I_4 &= \frac{1}{8} e^{-\pi^2} \sqrt{\pi} \left[2e^{\pi^2}\,\mathrm{Erf}(x) + \mathrm{i}\left(\mathrm{Erfi}(\pi - \mathrm{i}x) - \mathrm{Erfi}(\pi + \mathrm{i}x)\right)\right] \\
I_5 = I_6 &= \frac{1}{8} e^{-\pi^2} \sqrt{\pi} \left(2\,\mathrm{Erfi}[\pi] - \mathrm{Erfi}[\pi - \mathrm{i}x] - \mathrm{Erfi}[\pi + \mathrm{i}x]\right)
\end{aligned}
$$

This solution seems complicated, but its effect on the first term is small but important, see the picture[3]:

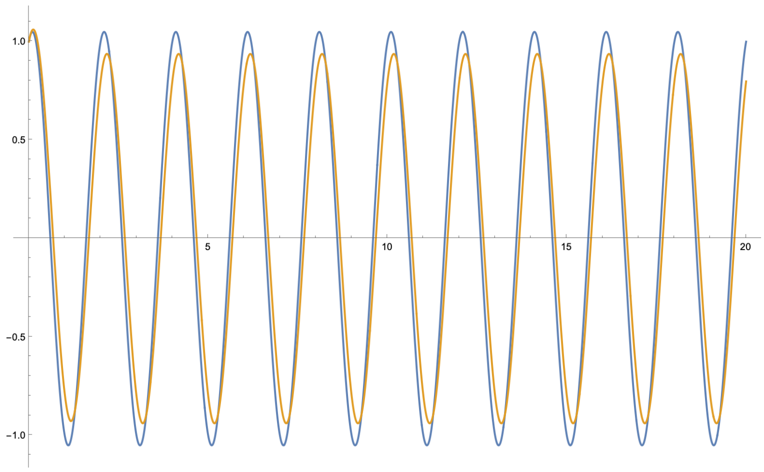

Figure 9: *In blue we have the first proposed solution, $y_0(x)$, which is a sum of sine and cosine. In orange, we plotted the $y(x) = y_0(x) + I$, being the main difference the reduction of the amplitude in all the function but at the beginning where it is a little bit higher.*

As we can see this approach repeats the solution and its behaviour of our first case. But me must to say that this way is harder than the case 1.

[2] All the following results where made using Wolfram Mathematica

[3] This plot was done with the solution of the integral previously calculated and by taking $A = \pi$

4 Summary

To sum up, this work focuses on analyzing and providing an analytical description of the non-linear stage of the Self-Modulation Instability (SMI), a phenomenon critical in plasma-based accelerators. The project is inspired by efforts like the AWAKE experiment, which seeks to use plasma wakefields to accelerate particles beyond current material limitations in accelerators.

Plasma-based particle acceleration holds great promise for achieving higher energy levels in particle accelerators without material breakdown, a limiting factor in traditional accelerators. This study aims to describe the nonlinear or saturation stage of the SMI, an instability in plasma that arises when the density of plasma electrons fluctuates due to the presence of a charged particle beam. In order to do so, we begin with deriving the linear wakefield theory, based on Maxwell's equations and the cold fluid approximation for the plasma. It describes how electromagnetic fields interact with plasma and beam particles. The Green's function method is proposed as a mathematical approach to solving the relevant differential equations.

The resonant frequency of the plasma wakefields depends on the oscillation amplitude, specifically influenced by the plasma density perturbation. This section presents an analytical attempt to solve the differential equations governing the system's behavior during this nonlinear stage using various mathematical techniques, including special functions and Green's method. Two different cases of the bunch's charge density profile are explore: constant and a gaussian-kind given by our before defined $f(x)$. We show that as we could expect the non-linear effects establish a start and end of the plasma density perturbation and the duration of the spread depends on the value of the σ of the particle bunch.

The study successfully formulates and analytically explores the nonlinear dynamics of the SMI in a plasma wakefield accelerator. Although the resulting equations are complex and often require numerical solutions, the methods presented contribute to understanding how plasma wakefields behave at the saturation stage of SMI, aiding future designs of high-energy particle accelerators. As a consequence of this study we encourage to explore a more sophisticated way of resolve and plot the **Mathieu's functions** in order to obtain smoother solutions.

References

[1] M. Turner, E. Walter, C. Amoedo, *et al.*, *Experimental observation of motion of ions in a resonantly driven plasma wakefield accelerator*, 2024. arXiv: 2406.16361 [physics.plasm-ph]. [Online]. Available: https://arxiv.org/abs/2406.16361.

[2] M. Moreira, "Properties of the hosing and self-modulation instabilities of long particle beams in overdense plasma," Presented 23 Jan 2024, University of Lisbon, 2023. [Online]. Available: https://cds.cern.ch/record/2891407.

[3] "Integral equations and green's functions," in *Applied Mathematical Methods in Theoretical Physics*. John Wiley Sons, Ltd, 2009, ch. 2, pp. 31–104, ISBN: 9783527627745. DOI: https://doi.org/10.1002/9783527627745.ch2. eprint: https://onlinelibrary.wiley.com/doi/pdf/10.1002/9783527627745.ch2. [Online]. Available: https://onlinelibrary.wiley.com/doi/abs/10.1002/9783527627745.ch2.

[4] É. Mathieu, "Mémoire sur le mouvement vibratoire d'une membrane de forme elliptique.," fre, *Journal de Mathématiques Pures et Appliquées*, vol. 13, pp. 137–203, 1868. [Online]. Available: http://eudml.org/doc/234720.

[5] D. B. Owen, "A table of normal integrals," *Communications in Statistics - Simulation and Computation*, vol. 9, no. 4, pp. 389–419, 1980. DOI: 10.1080/03610918008812164. eprint: https://doi.org/10.1080/03610918008812164. [Online]. Available: https://doi.org/10.1080/03610918008812164.